Genoves Guzman, B., Dowhuszko, A. A., Gil Jimenez, V. P. & Perez-Neira, A. I. (2018). Robust Cooperative Multicarrier Transmission Scheme for Optical Wireless Cellular Networks. *IEEE Photonics Technology Letters*, 30(2), pp. 197–200.

DOI: 10.1109/lpt.2017.2781184

Robust Cooperative Multicarrier Transmission Scheme for Optical Wireless Cellular Networks

Borja Genovés Guzmán, *Student Member, IEEE,* Alexis A. Dowhuszko, Víctor P. Gil Jiménez, *Senior Member, IEEE,* and Ana I. Pérez-Neira, *Senior Member, IEEE*

***Abstract*—Visible Light Communication (VLC) is a promising technology to achieve high data rates in heterogeneous scenarios. However, VLC strongly depends on the existence of a Line-of-Sight (LoS) link between transmitter and receiver to guarantee a good data rate performance, which is often a condition that is difficult to satisfy in practice. In this paper, a novel cooperative multicarrier transmission scheme is proposed, where neighboring attocells smartly cooperate to decrease the probability of blockage in the LoS link. This approach is compared to single-cell transmission schemes, obtaining notable gains in both received Signal-to-Interference-plus-Noise Ratio and cell data rate when blockage of the LoS link occurs towards the nearest Base Station.**

***Index Terms*—Cooperative transmission, co-channel interference, frequency reuse, joint transmission, LoS blockage, macro-diversity, Visible Light Communication.**

I. Introduction

THE mobile data traffic demand has been exponentially increasing during the last decade, and the Radio Frequency (RF) spectrum has become overcrowded to cope with this trend. Thus, new alternatives are being studied to satisfy the user demand. In this context, Visible Light Communication (VLC) raises as a suitable solution for guaranteeing the user expectations [1]. The level of maturity of solid state lighting technology has enormously improved during the last years, and halogen lighting is being replaced by Light-Emitting Diodes (LEDs) to save energy, protect the environment, and reduce the maintenance costs due to long lifetime. As nowadays LEDs can be modulated at very high data rates, the research community is leveraging this aspect to provide both data communication and indoor illumination at the same time.

VLC makes use of license-free electromagnetic spectrum that does not generate interference to co-located RF systems. The short-range coverage of the LED lighting allows the creation of a dense small cell network that increases the area spectral efficiency. Such a dense VLC network deployment is usually termed in the literature as an attocell network [2].

The front-end devices of a VLC system are tipically an LED and a PhotoDiode (PD), which take the role of transmitter and receiver, respectively. The LED is a non-coherent light source; thus, Intensity Modulation (IM) is employed to encode digital information. The PD detects optical intensity and converts it into an electrical signal; thus, Direct Detection (DD) is the term used on the receiver side. Optical modulation techniques with high spectral and energy efficiencies have been recently developed [3]. Among these, Direct-Current biased Optical Orthogonal Frequency Division Multiplexing (DCO-OFDM), Asymmetrically Clipped Optical OFDM (ACO-OFDM), and enhanced Unipolar OFDM (eU-OFDM) are the ones that have received most attention lately.

A limiting factor in the performance of an optical attocell network is the Co-Channel Interference (CCI) that is generated for using the same communication resources in adjacent attocells. Thus, many works have contributed to mitigate the CCI. For example, the authors of [2] and [4] apply joint transmission and fractional frequency reuse concepts to serve cell-edge users, respectively, improving the received signal quality and the achievable spectral efficiency. Similarly, the authors of [5] study spatial diversity techniques to improve the performance of the optical attocell system. Finally, Multiple-Input Multiple-Output techniques in the context of an optical attocell network are explored in [1] and [6].

Another limiting factor in VLC is the need of a Line-of-Sight (LoS) condition between LED and PD. In indoor scenarios with many pieces of furniture and users, LoS is often partially or completely blocked. To address this problem, in this letter we propose a novel approach that is suitable to combat the LoS link blockage in wireless systems using multicarrier modulation, including (but not limited to) VLC systems. For single-carrier modulation schemes like On-Off Keying (OOK), a scheme to improve the performance when LoS link blockage happens was already proposed in [7]. The benchmark for this work is established in [8].

II. System Model

Due to spectral efficiency reasons, DCO-OFDM is adopted in this paper. Nevertheless, the proposed scheme is extensible to any other multicarrier modulation scheme. In DCO-OFDM, subcarriers 0 and $K/2$ are zero-valued. In addition, the information transported on the second half of the subcarriers (with indexes from $K/2+1$ to $K-1$) are Hermitian symmetric with respect to the information transported on the first half (with indexes from 1 to $K/2-1$) to obtain a real-valued output signal in the time domain. Thus, the frequency-domain signal is $\mathbf{X}_{\mathrm{H}} = \left[0 \;\; \{X^t[k]\}_{k=1}^{K/2-1} \;\; 0 \;\; \{X^t[K/2-k]^*\}_{k=1}^{K/2-1}\right]$, where $X^t[k]$ is the symbol transmitted on the k-th subcarrier and $(\cdot)^*$ denotes the complex conjugate.

This work has been partially funded by the Spanish MECD FPU fellowship program granted to the author B. Genovés Guzmán, the Catalan Government under Grant 2014SGR1567, and the Spanish Government under the national project 'ELISA' with ID no. TEC2014-59255-C3-3-R and TEC2014-59255-C3-1-R.

B. Genovés Guzmán and Víctor P. Gil Jiménez are with the Department of Signal Theory and Communications of the University Carlos III of Madrid. Alexis A. Dowhuszko and Ana I. Pérez-Neira are with the Centre Tecnològic de les Telecomunicacions de Catalunya. Email: {bgenoves, vgil}@tsc.uc3m.es; {alexis.dowhuszko, ana.perez}@cttc.es.

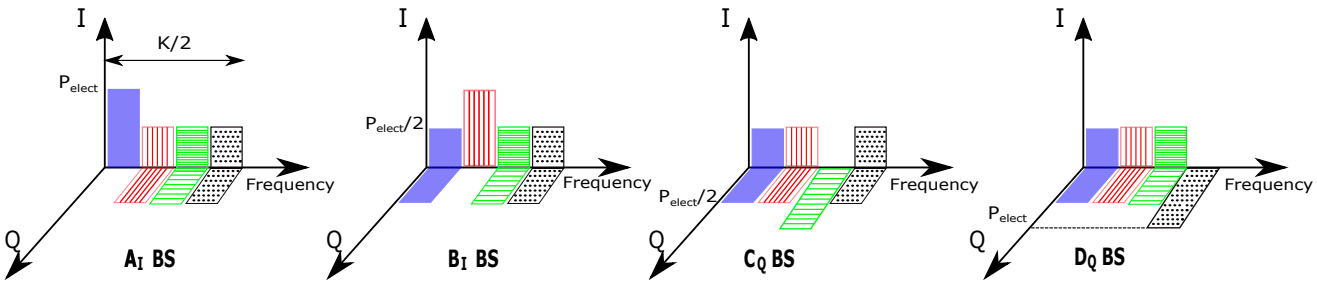

Fig. 1: Frequency bands assignment to four types of BS (A_I, B_I, C_Q, and D_Q). Equal optical power allocation is performed on all frequency bands.

A. Proposal

The goal is to mitigate the effect of LoS link blockage in crowded scenarios with a high density of obstacles (e.g., furniture). To cope with this, a cooperative scheme is proposed, where each user is always connected to an *anchor* Base Station (BS) and receives useful signal from other two neighboring BSs. Fig. 1 shows the frequency reuse among attocells, as well as the power distribution, among I-Q signal components. The first sub-band carries the information sent to the users located in the central target attocell (A_I). Note that there are 6 different sectors in the central cell of Fig. 2a where cooperation takes place within the target cell (A_I). Besides, it can be seen that only three different cells cooperate at the same time in any user position. For clarity purposes, the tessellation in Fig. 2a shows the edges for the reference *anchor* attocell, whereas the (blue) tessellation in Fig. 2b and Fig. 2c shows the cooperation edges of the corresponding attocells.

In order to reduce the inter-cell interference, bandwidth is divided into four sub-bands as it can be seen in Fig. 1 (reuse factor $\Delta = 4$). Each *anchor* BS uses one sub-band to serve its associated users, whereas cooperation is carried out in the other three sub-bands, cooperating with 2 neighboring attocells per sub-band (one in I and other in Q). In brief, each BS sends information to the users that lie in its own cell coverage area and, in addition, to the users that lie in the cooperative area that overlaps with the six neighboring attocells. In the time domain, each BS alternates the transmission of information to its associated user following an I, Q, and idle mode $(\emptyset)$ sequence, such that a cluster size of 12 is achieved (i.e., 4 frequency bands, 2 orthogonal I/Q signals, and 3/2 IQ-time hopping pattern). This transmission mode will change in time according to the pattern represented in Fig. 2b, such that no attocell remains without serving its users. Fig. 2c shows the BSs interfering to users located in the central target attocell. $\mathcal{S}_1$ contains the indexes of interfering BSs that use the same transmission resources with the same main sub-band (i.e., all attocells named A_I, represented with blue triangles in Fig. 2c), whereas $\mathcal{S}_2$ denotes the set of interfering BSs that use the same transmission resources but with different main sub-band (i.e., attocells B_I, B_Q, B_ϕ, C_I, C_Q, C_ϕ, D_I, D_Q, and D_ϕ, represented with yellow squares in Fig. 2c).

B. Analysis

The Signal-to-Interference-plus-Noise Ratio (SINR) is an important metric to evaluate the performance of a cellular system. An expression for the SINR that is obtained with our proposed scheme on subcarrier k is presented in (1), where $H_i(k)$ is the frequency response of the VLC channel on the k-th subcarrier received from the i-th BS, and $\eta_{\rm pd}$ and $\eta_{\rm led}$ are the responsivity of the PD and the electrical-to-optical conversion efficiency of the LED, respectively. The term $\sigma_{\rm x}^2$ denotes the electrical signal variance, and ρ is an attenuation factor related to the clipping effect that can be approximated as $\rho = Q(\lambda_{\rm b}) - Q(\lambda_{\rm t})$, where $\lambda_{\rm b}$ ($\lambda_{\rm t}$) is the normalized bottom (top) clipping levels, and $Q(x) = 1/\sqrt{2\pi}\int_x^\infty \exp(-u^2/2)du$. Similarly, $\xi = \sqrt{K/(K-2)}$ is a normalizing factor that compensates the absence of energy on subcarriers 0 and $K/2$. The clipping noise is approximated as Gaussian distributed with zero mean and variance $\sigma_{\rm clip}^2$ [8]. The receiver noise variance is $\sigma_{\rm rx}^2 = \frac{N_0 F_{\rm s}}{\xi^2}$, which is divided by 2 in (1) because it should be considered in only one dimension when real-valued symbols are used (either in I or Q component signals). $F_{\rm s}$ represents the sampling frequency.

Considering the equations for $|H_i(k)|^2$ and $\sigma_{\rm x}^2$ as stated in [8], the SINR can be simplified as

$$\gamma(k) = \left(\frac{\left(\rho^2 + \sigma_{\rm clip}^2\right)\mathcal{I} + \mathcal{Z}(k)}{\rho^2 \chi} + \frac{\sigma_{\rm clip}^2}{\rho^2 \xi^2} \right)^{-1}, \tag{2}$$

where

$$\mathcal{I} = \sum_{i \in \mathcal{S}_1} (r_i^2 + h^2)^{-m-3} + \sum_{i \in \mathcal{S}_2} \frac{1}{2}(r_i^2 + h^2)^{-m-3}, \tag{3}$$

$$\begin{aligned}\gamma(k) &= \frac{\eta_{\rm pd}^2 \eta_{\rm led}^2 \sigma_{\rm x}^2 \rho^2 \xi^2 \left(|H_0(k)|^2 + \frac{1}{2}\left(|H_1(k)|^2 + |H_2(k)|^2\right)\right)}{\eta_{\rm pd}^2 \eta_{\rm led}^2 \sigma_{\rm x}^2 \left(\sigma_{\rm clip}^2 \left(|H_0(k)|^2 + \frac{1}{2}\left(|H_1(k)|^2 + |H_2(k)|^2\right)\right) + \sum\limits_{i \in \mathcal{S}_1} \left(\rho^2 + \sigma_{\rm clip}^2\right)|H_i(k)|^2 + \sum\limits_{i \in \mathcal{S}_2} \frac{1}{2}\left(\rho^2 + \sigma_{\rm clip}^2\right)|H_i(k)|^2 \right) + \frac{1}{2}\sigma_{\rm rx}^2} \\ &= \left(\left(\frac{\rho^2 \xi^2 \left(|H_0(k)|^2 + \frac{1}{2}\left(|H_1(k)|^2 + |H_2(k)|^2\right)\right)}{\left(\rho^2 + \sigma_{\rm clip}^2\right)\left(\sum_{i \in \mathcal{S}_1} |H_i(k)|^2 + \sum_{i \in \mathcal{S}_2} \frac{1}{2}|H_i(k)|^2\right) + \frac{N_0 F_{\rm s}}{2\xi^2 \eta_{\rm pd}^2 \eta_{\rm led}^2 \sigma_{\rm x}^2}} \right)^{-1} + \frac{\sigma_{\rm clip}^2}{\rho^2 \xi^2} \right)^{-1}\end{aligned} \tag{1}$$

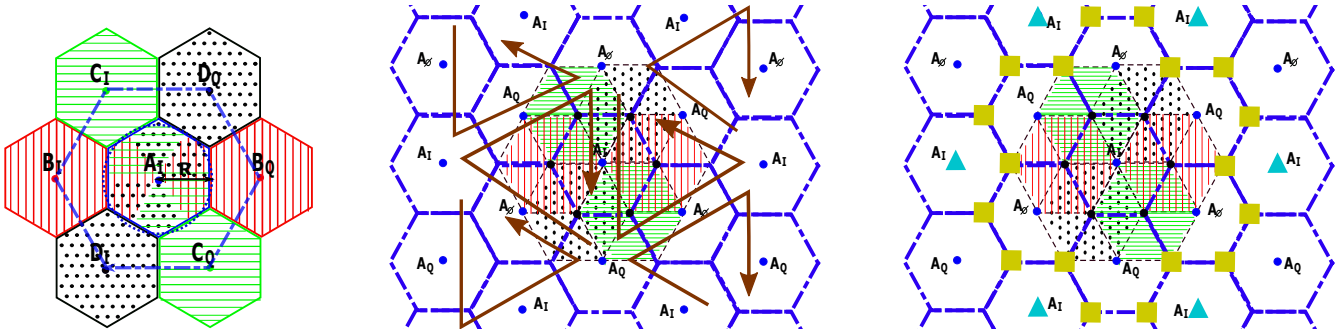

(a) Cooperative scenario for cell A_I. (b) I-Q hopping sequence among A_I, A_Q, A_ϕ modes. (c) Interfering BSs: triangles $\in \mathcal{S}_1$, squares $\in \mathcal{S}_2$.

Fig. 2: Proposed cooperative scenario using central cell A_I as reference: (a) Cooperation region of A_I with the six neighboring cells, (b) IQ-time hopping pattern among cells using the same band (A, in this case), (c) Localization of BSs that generate CCI for serving users not associated to the central reference cell.

$$\chi = \xi^2\Big((r_0^2+h^2)^{-m-3} + \frac{1}{2}(r_1^2+h^2)^{-m-3} + \frac{1}{2}(r_2^2+h^2)^{-m-3}\Big), \tag{4}$$

and

$$\mathcal{Z}(k) = \frac{K_{\mathrm{e/v}}^2 N_0(r) F_\mathrm{s} \exp\left(\frac{kF_\mathrm{s}}{KF_\mathrm{fe}}\right)(\zeta + \mathbb{E}\left[U(x(t))\right])^2}{2\left(\xi E_\mathrm{v} A_\mathrm{pd}\eta_\mathrm{pd} h^{m+3}\right)^2}. \tag{5}$$

In the previous equations, r_i is the horizontal distance between the user and the i-th BS, h is the vertical distance between the user and the BS, and m is the Lambertian emission order of the LED. The luminous efficacy is represented by $K_{\mathrm{e/v}}$, and $N_0(r)$ considers the combined effect of the shot noise (due to received signal and ambient light optical power) and thermal noise [8]. F_fe controls the front-end device bandwidth, and ζ is the ratio of DC-bias level (I_dc) to the electrical signal standard deviation (σ_x). $\mathbb{E}\left[U(x(t))\right]$ denotes the expected value of the data-carrying signal after clipping [9], which is approximated to 0 assuming a linear dynamic range from 0 to $2I_\mathrm{dc}$. As a consequence, $\lambda_t = -\lambda_b = \zeta$. A_pd is the PD physical area, and the cell center illuminance from the BS is defined as

$$E_\mathrm{v} = \frac{(m+1)\Phi_\mathrm{v}}{2\pi h^2} = \frac{(m+1)P_\mathrm{opt}K_{\mathrm{e/v}}}{2\pi h^2}, \tag{6}$$

where Φ_v is the output luminous flux of the luminary.

The probability that the downlink SINR is less than a threshold γ_th is computed as $\mathbb{P}[\gamma(k) < \gamma_\mathrm{th}] = \int_0^R f_r(r)\mathbb{P}[\gamma(k) < \gamma_\mathrm{th}|r]dr$, where $f_r(r) = \frac{2r}{R^2}$ when a uniform distribution of users is assumed within each cell and R is the circular cell radius. Since the CCI follows a periodic distribution with a period of 60° due to the central symmetric deployment of the interfering BSs, $\mathcal{I}$ can be estimated using the *flower* model as stated in [8] and [10]. Thus, the conditional probability $\mathbb{P}[\gamma(k) < \gamma_\mathrm{th}|r]$ is derived as

$$\mathbb{P}[\gamma(k) < \gamma_\mathrm{th}|r] = \mathbb{P}\left[\cos(6\theta) > \frac{2\rho^2\chi\left(\frac{1}{\gamma_\mathrm{th}} - \frac{\sigma_\mathrm{clip}^2}{\rho^2\xi^2}\right) - 2\mathcal{Z}(k)}{(\rho^2+\sigma_\mathrm{clip}^2)|\mathcal{I}_{30^\circ} - \mathcal{I}_{0^\circ}|} - \frac{\mathcal{I}_{30^\circ}+\mathcal{I}_{0^\circ}}{|\mathcal{I}_{30^\circ}-\mathcal{I}_{0^\circ}|}\Big| r\right], \tag{7}$$

where $\mathcal{I}_{30^\circ}$ and $\mathcal{I}_{0^\circ}$ are the interference of a user located at polar coordinates $re^{j\pi/6}$ and re^{j0}, respectively, which are computed using (3). By using Adaptive Modulation and Coding (AMC) schemes, the cell data rate of the proposed scheme can be obtained as

TABLE I: Adaptive Modulation and Coding SINR regions for a BER $= 10^{-3}$

$\epsilon[n]$ [bits/symbol]	1	2	3	4	5	6	7	8
$\mathrm{AMC_{QAM}}$: $\gamma_\mathrm{th}[n]$ [dB]	-	9.8	13.4	16.5	19.6	22.5	25.5	28.4
$\mathrm{AMC_{MAM}}$: $\gamma_\mathrm{th}[n]$ [dB]	7.6	14.0	19.8	25.5	31.3	37.1	43.0	48.9

$$s = \frac{F_\mathrm{s}}{\frac{3}{2}\Delta K}\sum_{k=1}^{K/2-1}\sum_{n=1}^{N}\epsilon[n]\Big(\mathbb{P}\big[\gamma(k) < \gamma_\mathrm{th}[n+1]\big] - \mathbb{P}\big[\gamma(k) < \gamma_\mathrm{th}[n]\big]\Big), \tag{8}$$

where the reuse factor $\Delta = 4$, and $\epsilon[n]$ is the spectral efficiency of the n-th AMC level that is obtained with a minimum required SINR for $\gamma_\mathrm{th}[n]$. The factor 3/2 in the denominator comes from the IQ-time hopping pattern shown in Fig. 2b.

III. Results

In this section, SINR and cell data rate performance evaluations are presented using [8] as baseline scheme. Two AMC schemes [11] are used to calculate the cell data rate, as illustrated in Table I: uncoded QAM ($\mathrm{AMC_{QAM}}$) and uncoded M-ary Amplitud Modulation ($\mathrm{AMC_{MAM}}$). In all figures, the proposed Multi-Cell transmission scheme with Frequency Reuse factor 4 is referenced as MCFR4, whereas the baseline Single-Cell transmission schemes with Frequency Reuse factor 1 and 3 are referenced as SCFR1 and SCFR3, respectively.

The Lambertian emission order of the LED was selected to verify $m = \frac{\ln \sigma_\mathrm{P}}{\ln\left(1+\frac{R^2}{h^2}\right)} - 3$, such that the power decrease factor (σ_P), that measures the relation between the received optical power at the cell center and cell edge, equals 12 dB. The vertical separation h was set to 2.25 m, the receiver field of view is 90°, and a sampling frequency $F_\mathrm{s} = 50$ MHz was chosen to minimize the effect of the low-pass filtering of the LED [8]; this way, the equivalent electrical channel is identical for all frequency sub-bands. The front-end device bandwidth factor F_fe is 31.7 MHz, and the number of subcarriers (K) is equal to 512. Moreover, $\eta_\mathrm{pd} = 0.4$ A/W, $A_\mathrm{pd} = 1\,\mathrm{cm}^2$, $K_{\mathrm{e/v}} = 100$ lm/W, $\zeta = 5.05$ dB, and $E_\mathrm{v} = 500$ lux. Similarly, Φ_v is calculated from (6). Relevant parameters to compute $N_0(r)$ [8] are the illuminance from ambient light, the absolute temperature and the receiver load resistance, configured as 100 lux, 300 K and 500 Ω, respectively.

Fig. 3 depicts the Cumulative Distribution Function (CDF) of the SINR at DC for the SCFR1, SCFR3 and MCFR4

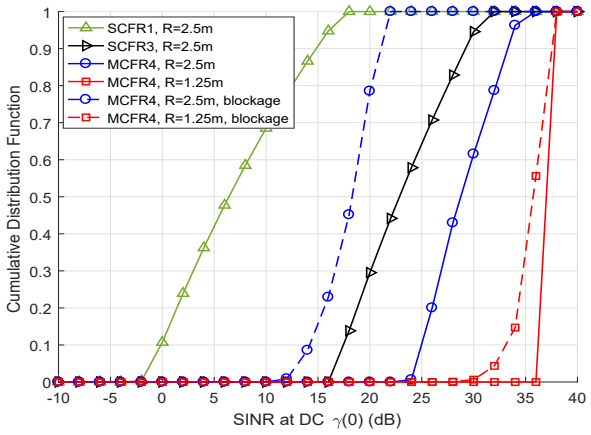

Fig. 3: Cumulative Distribution Function of the SINR at DC for different transmission schemes, cell radii, and LoS blockage conditions.

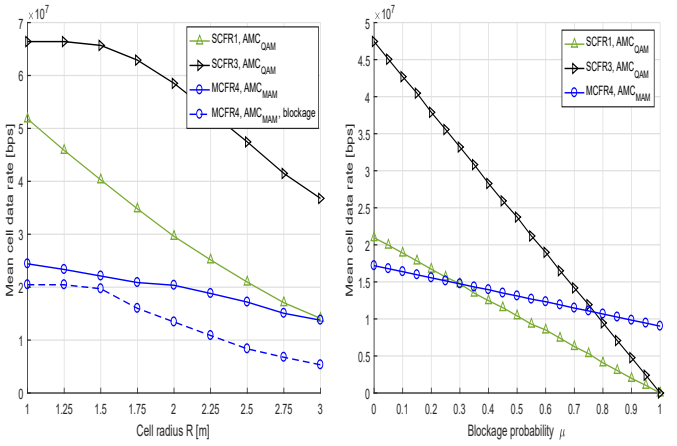

(a) Mean cell data rate versus cell radius (R).

(b) Mean cell data rate versus blockage probability ($R = 2.5$m).

Fig. 4: Effect of the Cell Radius (R) and the LoS link Blockage Probability (μ) in the mean cell data rate of the different transmission schemes .

schemes. As expected, the larger the reuse factor, the better the SINR performance, as the CCI power decreases. Note that when there is a LoS link blockage towards the serving (*anchor*) BS, the SINR of SCFR1 and SCFR3 vanishes and, due to that, they are not plotted. Differently, the proposed MCFR4 scheme can provide an acceptable SINR even when the LoS link is blocked. The smaller the size of the attocell, the lower the loss with respect to the LoS case is, because the power received from cooperating cells improves (compared to the CCI).

Results of cell data rate are presented in Fig. 4. Note that the AMC_{QAM} cannot be used in MCFR4 because useful information to each user is transmitted over only one signal component (either I or Q). Due to that, the AMC_{MAM} scheme is applied. As shown in Fig. 3, the larger the cell radius (R), the worse the SINR in reception and the lower the cell data rate in Fig. 4a is. The SCFR3 scheme manages the interference well and, due to that, it achieves a better cell data rate when compared to SCFR1.

The proposed MCFR4 scheme gets lower cell data rate for using an MAM AMC scheme instead of QAM AMC, besides the additional $3/2$ reuse factor for applying the I-Q rotation sheme shown in Fig. 2b. However, it is important to highlight that MCFR4 is the only scheme that guarantees connectivity to all users even in presence of LoS link blockage. The performance loss of SCFR3 and MCFR4 with blockage for radii beyond 1.5 m is produced because the likelihood of selecting an AMC mode below the 8-th and 5-th, respectively, is not negligible anymore (See Fig. 3 and Table I). Fig. 4b shows the robustness of the proposed MCFR4 scheme against the blockage probability. Let us assume that μ is the probability of blockage towards the serving (*anchor*) BS; then, the cell data rate of MCFR4 is higher than the one obtained with SCFR1 (SCFR3) for values beyond $\mu = 0.3$ ($\mu = 0.75$). As expected, the variability of the mean cell data rate is lower for the MCFR4 scheme due to the macro-diversity that is exploited due to cooperation in the attocell network.

IV. Conclusion

In this letter, a new approach to combat the LoS blockage in indoor VLC systems was presented, which is a typical impairment in indoor scenarios. A cooperating scheme was proposed, where neighboring BSs jointly coordinate their transmission using DCO-OFDM. In absence of LoS link blockage, the obtained SINR performance at DC is better than the one obtained with transmission techniques without cooperation. Concerning the mean cell data rate, it was observed that it decreases due to the use of a larger cell cluster size and uncoded MAM AMC. When LoS link blockage occurs, the SINR performance decreases but, in return, it is possible to guarantee a minimum data rate to all active users in the system (as opposed to single-cell transmission schemes).

References

[1] L. Zeng, D. C. O'Brien, H. L. Minh, G. E. Faulkner, K. Lee, D. Jung, Y. Oh, and E. T. Won, "High data rate multiple input multiple output (MIMO) optical wireless communications using white led lighting," *IEEE J. Sel. Areas Commun.*, vol. 27, no. 9, pp. 1654–1662, Dec. 2009.

[2] C. Chen, D. Tsonev, and H. Haas, "Joint transmission in indoor visible light communication downlink cellular networks," in *Proc. IEEE Globecom Workshops*, Dec. 2013, pp. 1127–1132.

[3] J. Armstrong, "OFDM for Optical Communications," *J. Lightw. Technol.*, vol. 27, no. 3, pp. 189–204, Feb. 2009.

[4] C. Chen, N. Serafimovski, and H. Haas, "Fractional frequency reuse in optical wireless cellular networks," in *Proc. IEEE Personal, Indoor and Mobile Radio Commun. Symp.*, Sept. 2013, pp. 3594–3598.

[5] Z. Chen and H. Haas, "Space division multiple access in visible light communications," in *Proc. IEEE Int. Conf. Commun.*, June 2015, pp. 5115–5119.

[6] A. H. Azhar, T. A. Tran, and D. O'Brien, "A Gigabit/s Indoor Wireless Transmission Using MIMO-OFDM Visible-Light Communications," *IEEE Photon. Technol. Lett.*, vol. 25, no. 2, pp. 171–174, Jan. 2013.

[7] B. G. Guzman, A. L. Serrano, and V. P. G. Jimenez, "Cooperative optical wireless transmission for improving performance in indoor scenarios for visible light communications," *IEEE Trans. Consum. Electron.*, vol. 61, no. 4, pp. 393–401, Nov. 2015.

[8] C. Chen, D. A. Basnayaka, and H. Haas, "Downlink performance of optical attocell networks," *J. Lightw. Technol.*, vol. 34, no. 1, pp. 137–156, Jan. 2016.

[9] S. Dimitrov, S. Sinanovic, and H. Haas, "Clipping Noise in OFDM-Based Optical Wireless Communication Systems," *IEEE Trans. Commun.*, vol. 60, no. 4, pp. 1072–1081, Apr. 2012.

[10] B. Almeroth, A. J. Fehske, G. Fettweis, and E. Zimmermann, "Analytical interference models for the downlink of a cellular mobile network," in *Proc. IEEE Globecom Workshops*, Dec. 2011, pp. 739–743.

[11] F. Xiong, *Digital Modulation Techniques, Second Edition (Artech House Telecommunications Library)*. Norwood, MA, USA: Artech House, Inc., 2006.